Model for the eruption of the Old Faithful geyser, Yellowstone National Park

Kieran D. O'Hara, *Dept. of Earth and Environmental Sciences (emeritus) University of Kentucky, Lexington, Kentucky 40506, USA, kieran.ohara@uky.edu; and* **E.K. Esawi,** *Division of Physical Sciences, Elizabethtown Community & Technical College, Elizabethtown, Kentucky 42701, USA*

ABSTRACT

A physical model of the Old Faithful geyser successfully replicates the eruption interval for the years 2000–2011. It is based on convective boiling in the conduit in three stages, and the model is in good agreement with published time-temperature-depth data. The preplay phase, which triggers the main eruption, displays a Rayleigh probability density function with a mode at nine minutes, and it plays an essential role in determining the main eruption interval. It is assumed that temperature gradients are small due to convection, and individual convection cells can be assigned a single heat content. Based on previous observations and drill-hole measurements, the bottom heating and recharge temperatures are assumed to be 110 °C and 80 °C, respectively, and the total volume of the cylindrical conduit is 23 m^3. A prescription for both short and long eruption intervals is

eruption interval = (time to boiling of upper stage) + (preplay time).

A composite model reproduces the bimodal eruption pattern in which long eruption durations are followed by long eruption intervals and short eruption durations are followed by short eruption intervals. The cause of short eruption durations is not addressed and remains unresolved.

INTRODUCTION

The Old Faithful geyser, an icon of the American West, has been studied for more than a century (Hayden, 1872). In 2010, 3.6 million tourists visited the Yellowstone National Park, Wyoming, for a total of 170 million visits since the park was established in 1872, indicating an enduring curiosity by the public in geyser activity. The geyser is not as regular as is commonly thought, because the eruption interval is bimodal and has varied over time (Rinehart, 1980). For example, in 1948 the mean eruption interval was 64 minutes (Birch and Kennedy (1972), in 1979 it was ~80 minutes (Kieffer, 1984), and in 2011 it was ~92 minutes (GOSA, 2011). This pattern is attributed to earthquake activity and its effect on the local hydrology. Lengthening of the eruption cycle and other changes in geyser activity have been documented following major earthquakes in 1959, 1983, and 2002 (Rinehart, 1972; Hutchinson, 1985; Husen et al., 2004). Decadal and seasonal variations in the eruption interval have also been ascribed to variations in the hydrological cycle in Yellowstone (Hurwitz et al., 2008).

Several models have been proposed for geysers (Steinberg et al., 1978; Steinberg, 1980; White et al., 1967; Murty, 1979; Rinehart, 1980; Ingebritsen and Rojstaczer, 1993, among others) and for the Old Faithful geyser in particular (Rinehart, 1965, 1969; Fournier, 1969; Kieffer, 1984, 1989; Dowden et al., 1991; Kedar et al., 1998). These studies provide substantial insight into the eruption dynamics of geysers in general. The goal of our study is to present a new physical model for the observed eruption interval of Old Faithful over a continuous period of time for which we have interval data (both logbook and electronic) as well as duration and preplay times. Our model differs from previous studies in that the heating mechanism of the water occurs by convective boiling in three stages; in addition, the length of the preplay phase plays a central role in modeling the geyser eruption interval. Our study is based on data for the twelve-year period 2000–2011. Because the data are averaged over time, changes in the eruption interval with time due to intermittent or short-term effects (e.g., earthquakes or climate effects) are not addressed. The raw data for this study were provided by the Geyser Observation and Study Association's website at http://gosa.org/ofvclogs.aspx (GOSA, 2011).

ERUPTION CYCLE

The eruption cycle can be divided into three phases:
1. The eruption duration (2–5 min.);
2. The eruption interval (or recharge phase, 55–120 min.); and
3. The preplay phase (small, discrete eruptions lasting 1–35 min.).

The eruption itself can be subdivided into three stages:
1. Initiation and unsteady flow;
2. Steady flow; and
3. Decline (Kieffer, 1984).

The bimodal eruption pattern for the years 2000–2011 is shown in Figure 1. The eruption interval shows a major mode at ~92 minutes and a subsidiary mode at ~60–65 minutes (Fig. 1A). The eruption duration for the same period shows a mode at 4–4.5 minutes with the shorter duration events (2–2.5 minutes) being relatively rare, accounting for ~5% of all eruptions (Fig. 1B).

The eruption interval shows a pattern whereby short eruption durations are followed by short recharge intervals, and long eruption durations are followed by long recharge intervals; this pattern has been explained by the geyser's seismicity (Rinehart, 1965). Seismic noise produced by Old Faithful is interpreted in terms of the dynamics of vapor bubble formation (and collapse) during boiling in the conduit (Kieffer, 1984, 1989; Kedar et al., 1996, 1998; Cros et al., 2011). That seismic activity resumes almost
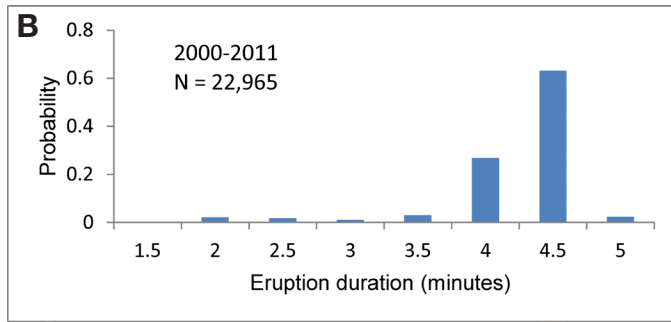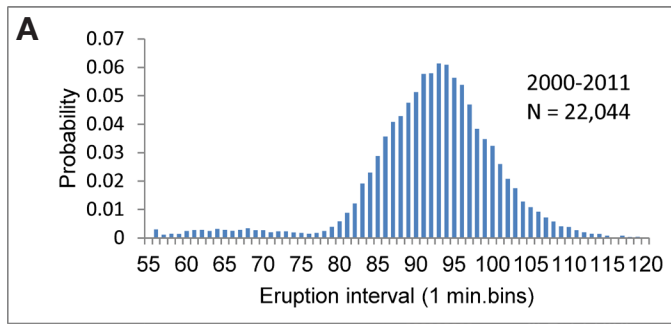
Figure 1. Probability histograms for eruption interval (A) and eruption duration (B) for the years 2000–2011 for Old Faithful. Electronic interval data (GOSA, 2011) for this time period agree with the log book data to within 1 min. when weekly averages are compared.
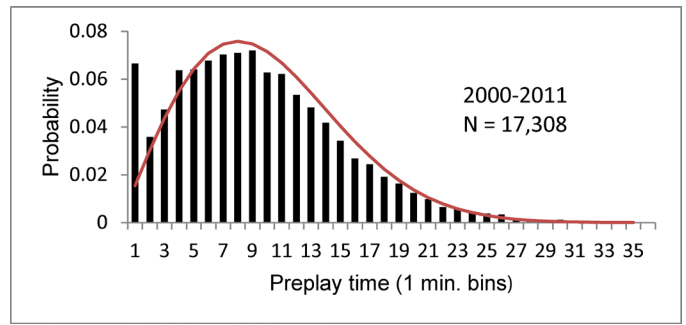

Figure 2. Probability histogram for the preplay eruption length for the years 2000–2011. The data have a mode at 9 min. (standard deviation [s.d.] = 5.6 min.). The distribution can be best modeled by a single parameter Rayleigh probability density function (Eq. 1 in text) with a mode at $\sigma = 9$ min. (s.d. = 5.2) for $x \geq 0$. The anomaly in the data at 1 min. is inferred to be an artifact of observation.

modeled using a single parameter Rayleigh probability density function ($x > 0$)

$$f(x, \sigma) = \frac{X}{\sigma^2} e^{-\frac{x^2}{2\sigma^2}}. \tag{1}$$

with a mode (σ) at nine minutes and a standard deviation of 5.2 minutes (solid curve, Fig. 2). The anomalously large number of one-minute preplay events is attributed to assigning some of the unsteady initiation stage to a short preplay event. In general, Rayleigh distributions have been used to model, among other phenomena, the height of ocean waves and wind velocities (e.g., Abd-Elfattah, 2011). The Rayleigh function fit indicates that the preplay eruptions are discrete random events.

PHYSICAL MODEL

Conduit Geometry

A variety of Old Faithful conduit shapes have been proposed to account for aspects of its eruption characteristics or filling history (Geis, 1968; Rinehart, 1980; Kieffer 1984). Based on down-hole video camera observations, Hutchinson et al. (1997) indicate that the immediately accessible conduit is an irregularly shaped enlarged east-west–trending fracture ~22 m deep. A constriction exists at ~7 m, above which the water level does not rise, except during preplay and the main eruption itself—presumably because an overflow outlet exists at this depth, possibly connected to the adjacent Firehole River (Rinehart, 1980). For simplicity, we assume here that the conduit is cylindrical with a cross sectional area of 1.5 m² for a total volume of ~23 m³ (23,000 liters) (Fig. 3). The conduit recharge phase is divided, for the purposes of calculation and for comparison with the data of Birch and Kennedy (1972), into three stages (S_1, S_2, and S_3), each with a height of 5 m and a volume of 7.7 m³ (7,700 liters). As discussed later, our model is not particularly sensitive to the details of the conduit geometry.

Water Temperatures and Recharge Rate

The data of Birch and Kennedy (1972) are still the most important time-temperature-depth information available for Old Faithful—and their Figure 5 is recast here in Figure 4. This diagram reveals in-phase heating and cooling episodes at different depths superimposed on an overall heating trend, which we interpret to be due to three distinct convection cells in the conduit

immediately after short-duration eruptions, but takes substantially longer to resume after long eruptions, is consistent with the idea that it takes longer for the water to recharge and come to a boil after a long eruption (resulting in a seismic quiet period), whereas after a short eruption, the water remaining in the conduit is still boiling and emits seismic noise throughout the recharge phase (e.g., Kieffer, 1984).

PREPLAY PHASE

The preplay phase consists of discrete splashes (each several meters in height lasting a few seconds) and precedes the main eruption. For example, observations of five consecutive eruptions on live video in May 2012 showed the following preplay lengths (in minutes) with the number of discrete splashes in parentheses: 17 (17); 10 (9); 12 (16); 13 (15); and 20 (18), suggesting that preplay events occur on average about once a minute. It has long been inferred that these discrete events trigger the main eruption by bringing the water in all or part of the conduit onto the boiling curve by reducing hydrostatic pressure in the water column (Bunsen, 1845, quoted in Allen and Day, 1935, p. 210), and this idea is still accepted (e.g., Kedar et al., 1998). For the most part, the discrete nature of these smaller eruptions is easily distinguished from the main eruption phase. However, in the case of very short preplay times, it becomes a judgment call whether the unsteady initiation of flow is part of the main eruption itself or represents a short preplay event—this would overestimate the number of short preplay events.

The length of the preplay phase was calculated by subtracting the time of the beginning of preplay from the beginning of the main eruption (Fig. 2). The preplay distribution shows a mode at nine minutes with a standard deviation of 5.6 minutes, and the distribution is skewed to the right. This distribution can best be
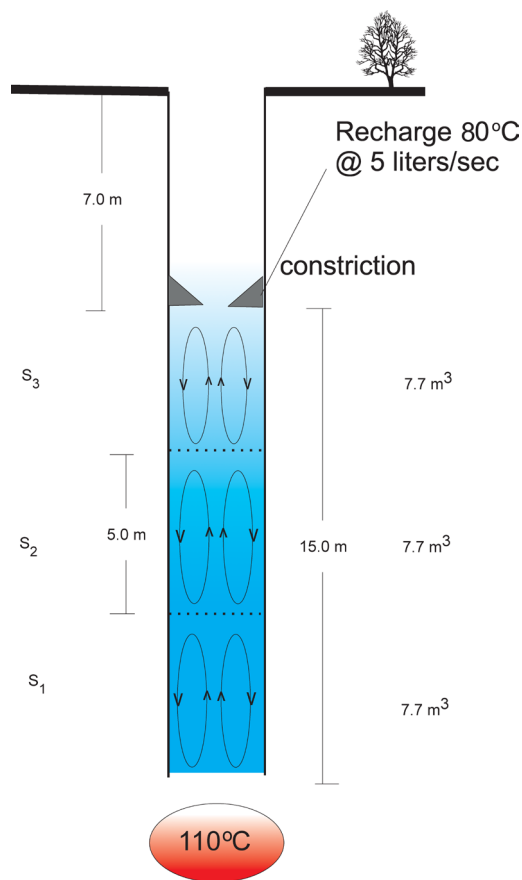
Figure 3. Idealized cylindrical model (radius 0.7 m) for the Old Faithful conduit to a depth of ~22 m with a total volume of 23 m³. The recharge water temperature is assumed to be 80 °C, and the bottom source temperature is assumed to be 110 °C. Recharge of the conduit occurs in three equal stages: S_1, S_2, and S_3. Convection cells are based on Figure 4.

Figure 4. Time-temperature plot for a single Old Faithful eruption at four depths (6, 12, 18, and 21 m) based on Figure 5 *in* Birch and Kennedy (1972). The in-phase cooling and heating at three different depths is interpreted to be due to convective mixing (see Fig. 3). The data indicate that the temperature in individual convection cells is not homogenized over time. Best-fit lines indicate an overall heating trend.

(Fig. 3). The data of Birch and Kennedy (1972, their fig. 5) also show a maximum temperature of 116 °C at the deepest levels, and Rinehart (1969, his fig. 1) observed a maximum temperature of ~110 °C during two eruption cycles (but his depth estimate of 30 m may be in error). Over a period of ~30 minutes before an eruption, Hutchinson et al. (1997) also observed water temperatures of ~110 °C near the bottom of the conduit; they interpreted temperature oscillations to be due to convection. Drilling in the Upper Geyser Basin, to which Old Faithful belongs, showed bottom hole temperatures at a depth of 20 m of 90 °C (Y-7 hole); 135 °C (Y-8); 120 °C (Y-1); and 125 °C (Carnegie I) (White et al., 1975), for a mean temperature of 118 °C at a depth equivalent to the base of the Old Faithful conduit. Based on geo-chemical arguments and water salinity, Fournier (1979, his fig. 7) indicated the existence of a parent water source of ~200 °C for the Upper Basin at depth, but such a high temperature has not been measured in the accessible conduit of Old Faithful.

The lowest temperature observed by Hutchinson et al. (1997) was 86 °C and is interpreted to be due to recharge water percolating into the conduit from shallower levels. Drilling in the Upper Geyser basin also indicates bottom hole rock temperatures at a depth of 7 m in the range of 60–100 °C (White et al., 1975). The lowest temperature reported by both Birch and Kennedy (1972, their fig. 5) and Rinehart (1969, his fig. 1) was 93 °C.
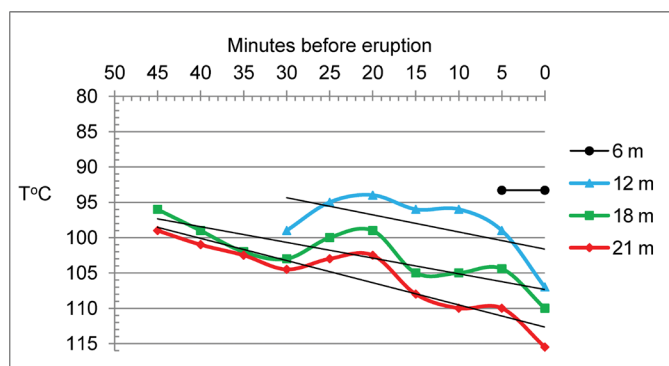
Based on these data, a temperature of 110 °C is taken here as the temperature of the heat source at the base of the observable conduit, and the temperature of the recharge water is assumed to be 80 °C. A constant recharge rate of 5 liters per second is also assumed, based on the total volume of discharge and the recharge time (Kieffer, 1984); this rate would fill the conduit up to the 7-m level in ~77 minutes. A constant recharge rate is a reasonable approximation because the hydrostatic pressure in the conduit shows an approximately linear profile over most of the recharge cycle (Hutchinson et al., 1997, their fig. 5A).

Lumped Capacitance Assumption

The process of filling a conduit from above with cold water and heating it from below at the same time produces an inherently unstable situation. The difference in density of water at 110 °C compared to 80 °C is ~20 kg/m³, which produces sufficient buoyancy to overcome viscous forces (i.e., high Rayleigh numbers), leading to convective overturn (Murty, 1979). The temperature variations plotted in Figure 4, and those observed by Hutchinson et al. (1997; their fig. 6) are attributed to vigorous convective overturn and mixing of parcels of hot and cold water. In the context of convection, Newton's law of cooling relates the heating rate (dQ/dt in W/m²) to the difference in temperature between the source temperature and the ambient temperature of the water (ΔT) at a given pressure:

$$dQ/dt = hA\Delta T, \qquad (2)$$

where h is the convective heat transfer coefficient (W/m^2K) and A is the cross sectional area of the conduit (1.5 m²).

If convection dominates over heat conduction and the water within individual convection cells is well mixed so that thermal gradients become small, the average thermal energy (Q) of each stage can be specified—it is simply related to temperature (T) by the specific heat capacity(C): $dQ/dT = C$ (kJ/kg). This is termed the Lumped Capacitance Assumption (Incropera and DeWitt, 2005, p. 240), and because of the vigorous convective mixing observed in the conduit, this approximation appears to be justified. The change in heat energy with time is then $dQ/dt = CdT/dt$. Substituting this relationship into equation (2) gives the change in temperature with time:

$$d(\Delta T)/dt = \frac{hA}{C}\Delta T, \qquad (3)$$

and the solution to equation (3) is

$$\Delta T = \Delta T_o e^{-kt}, \qquad (4)$$

where ΔT_o is the temperature difference at time $t = 0$ and the constant $k = hA/mC$, where m is the mass of the water. It is assumed that at the end of each recharge stage the reservoirs are well mixed due to convection and each stage can be assigned a single heat content and a temperature. This allows the thermal evolution of each stage to be modeled individually using the Lumped Capacitance Assumption.

Nucleate Boiling

During convection, rising parcels of hot water will spontaneously boil at lower water pressures. Vapor bubbles nucleate and rise, causing liquid mixing, effectively transporting heat upward. On reaching the cooler water, the rising bubbles collapse and give up their heat to the surrounding water (collapsing bubbles also then produce the seismic noise referred to earlier). These processes are referred to as nucleate boiling, and it is a very effective heat transfer mechanism (Incropera and DeWitt, 2005, p. 599).

Because of the complexity of analytical solutions during nucleate boiling, values for the convective heat transfer coefficient h are usually derived empirically. Experimental evidence indicates that h increases as ΔT in equation (2) increases, where ΔT is now the difference between the boiling temperature and the heating source temperature. The experiments indicate that nucleate boiling occurs when ΔT is 5 °C to 30 °C and produces values of dQ/dt in the range of 10^4–10^6 (W/m^2); when $\Delta T = 10$ °C, $dQ/dt \approx 10^5$ (Incropera and DeWitt, 2005, p. 598).

In the present case, nucleate boiling would occur if a parcel of water at 11 m depth (boiling point of 105 °C) rose to a depth of ~7.5 m in the conduit (boiling point of 95 °C). Direct evidence in support of this process comes from the existence of superheated geyser waters throughout Yellowstone National Park (Allen and Day, 1935, their table 3; Bloss and Barth, 1949) and Old Faithful itself (Hutchinson et al., 1997). A preliminary estimate for the value of h can be made by taking ΔT in equation (2) as 10 °C, based on the example above, which corresponds to a value of dQ/dt of 10^5 (W/m^2) based on experimental data. This produces a value for h of 6.6×10^3 W/m^{2}K. A value approximately twice this amount, 1.2×10^4 W/m^{2}K, produces the best fit to the data of Birch and Kennedy (1972) in the following models, and this value is used here (Table 1). The sensitivity of our model to this value is discussed later.

MODEL RESULTS

Figure 5 shows the temperature versus time evolution for each of the three stages using equation (4). Stage one (S_1) begins filling at $t = 0$ at a rate of 5 liters per second, and this takes ~25 minutes, at which time S_2 begins to fill. This takes an additional 25 minutes, after which time S_3 begins to fill; all three stages are full after ~77 minutes. The temperature at each stage increases with time from its initial value of 80 °C. Stage 1 is heated from below at

Table 1. Model Parameters

Parameter	Symbol	Value
Third stage volume	S_3	7.7 m^3
Second stage volume	S_2	7.7 m^3
First stage volume	S_1	7.7 m^3
Recharge rate		5 liters/sec
Recharge temperature		80 °C
Source temperatures		110 °C (S_1); 105 °C (S_2); 99 °C (S_3)
Specific heat capacity	C	4.18 kJ/kg
Conduit area	A	1.5 m^2
Convective heat transfer coefficient	h	1.2×10^4 W/m^{2}K

110 °C. Stage 2 is heated from below at 105 °C, which is the mean temperature of S_1 during S_2 filling. Stage 3 is heated from below at 99 °C, which is the mean temperature of S_2 during S_3 filling.

Two methods of heating were used—one heated the entire volume of water at each stage (7.7 m^3) as a function of time (Fig. 5, solid curves), and the second method heated the water while incrementally increasing the volume by 5 liters per second (Fig. 5, dashed color curves). The incremental heating produces an initial rapid temperature rise in the early part of the heating history, but after ~25 minutes, the two curves converge for each stage. Also shown on Figure 5 are the best fit lines from Figure 4 at different depths, based on the data of Birch and Kennedy (1972). Both heating methods produce a good fit to the data in the later part of the heating history. This allows a constant value for the mass of water (m) to be used in equation (4) (Fig. 5, solid curves). From a thermodynamic point of view, because enthalpy is a state function (Smith, 2005), the final temperature of each stage is independent of the heating path so that both heating methods produce the same final result.

The temperature of the water at each stage as a function of depth and time can be evaluated from Figure 5. Figure 6 shows the temperature of S_1, S_2, and S_3 at 75 minutes and at 85 minutes into the recharge phase. Also shown in Figure 6 is the reference boiling point curve (solid heavy line) and the depth-temperature curve of Birch and Kennedy (1972) 2.5 minutes before eruption (dashed heavy line). After 75 minutes into the recharge phase, all three stages are below the boiling curve, but at 85 minutes the uppermost stage (S_3) has reached boiling.
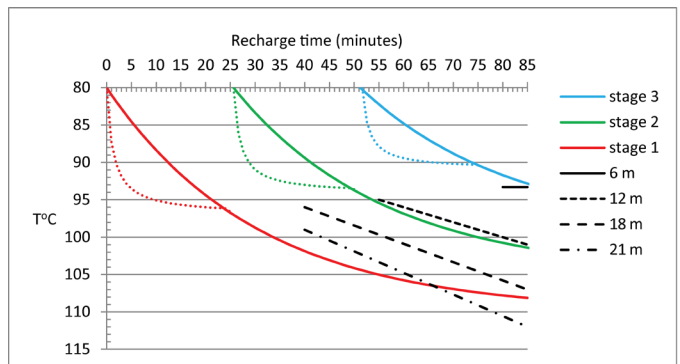

Figure 5. Temperature evolution with time (solid curves) for the three stages, based on equation (4) in the text using the parameters in Table 1. Stage 1 begins filling at $t = 0$, followed by stage 2 at ~25 min. and stage 3 at ~50 min. The colored dashed curves indicate the heating path when the conduit is incrementally filled at a rate of 5 liters/s, using equation (4). After ~25 min. into each stage, both solid and dashed curves converge and become identical. The best fit lines from Figure 4 at different depths are indicated—the heating curves are a good fit to the data.
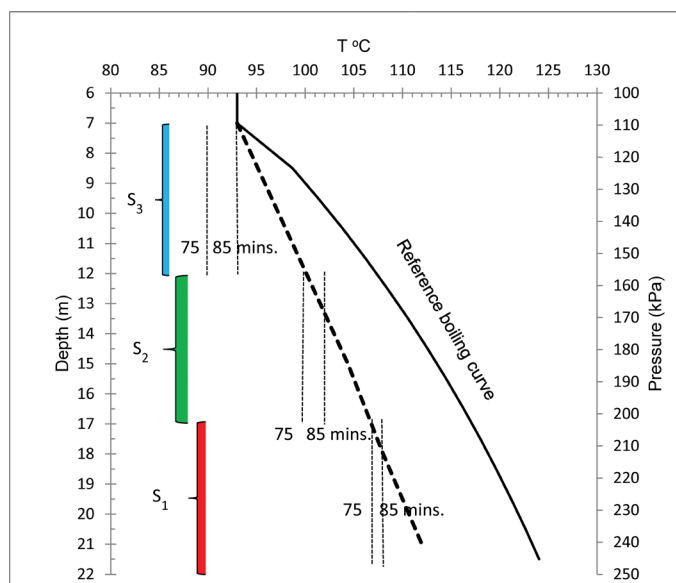
Figure 6. Temperature in the conduit after 75 and 85 min. (vertical dashed lines), based on Figure 5, relative to the boiling curve. The water boils at 93 °C at the park elevation (2246 m). The uppermost stage (S_3) intersects the boiling curve after 85 min. The heavy dashed curve represents the data of Birch and Kennedy (1972), 2.5 min. before eruption. The temperature in each stage after 85 min. is consistent with these data.

The middle and lower stages are still below the boiling curve at 85 minutes, consistent with the Birch and Kennedy (1972) data 2.5 minutes before the eruption.

Long and Short Eruption Intervals

Boiling at the top of the upper stage (S_3) will cause small amounts of water to be emitted at ground level, thereby reducing the pressure on deeper water, which in turn causes more boiling at deeper levels (Kieffer, 1989)—this is the beginning of the preplay phase. The net result of these small emissions is that the pressure reduction propagates downward until all the water column is at or above boiling—this triggers the main eruption phase, which occurs according to the following recipe:

Eruption interval = refill and boiling time for
S_3 + preplay time (Rayleigh distribution).

Refill and boiling time after a long eruption for S_3 is typically 85 minutes, based on our model (Fig. 5). The pressure data of Hutchinson et al. (1997) shows a pressure drop of 0.2 bars (20 kPa) immediately before an eruption, corresponding to the emission of 2 m of water (or about 3000 liters). This pressure drop is interpreted to be part of the preplay phase that triggered the main eruption.

Short eruption intervals follow short eruptions. This is usually rationalized on the basis that short eruptions expel smaller amounts of water and therefore the conduit takes a shorter time to recharge and heat to boiling before the next eruption. For illustration purposes (Fig. 7), it is assumed here that short eruptions involve only the second and third stages (S_2 and S_3), but any large fraction of the total volume could be expelled. If a short eruption expels these two stages, the remaining contents (namely, S_1) continue to heat toward boiling. Because the water level is well
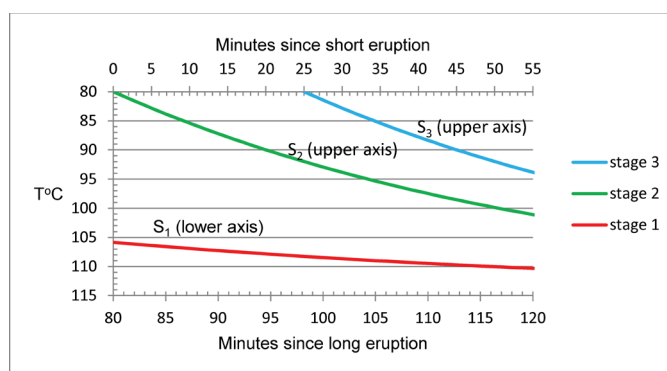

Figure 7. Temperature-time evolution of the upper stage (S_3) and middle stage (S_2) after a short eruption (upper axis) and the temperature-time evolution of the lower stage (S_1) after a long eruption (lower axis). The upper stage takes only 55 min. to reach boiling, which begins the preplay stage. Preplay activity triggers a full eruption, as described in the text.

below the surface, this continuous boiling will not produce any preplay activity. The continuous boiling accounts for the continuous seismic noise after a short eruption but absent after a long eruption (Kedar et al., 1998). After a short eruption, the second stage will begin to refill and heat as before, followed 25 minutes later by the uppermost stage.

Figure 7 shows the temperature evolution of all three stages after a short eruption using the same parameters as before (Table 1). The upper axis refers to the time after a short eruption for S_2 and S_3, whereas the lower axis refers to the time after a long eruption for S_1. The upper stage (S_3) reaches boiling (~93 °C at this elevation) within 55 minutes. This boiling initiates the preplay phase, causing S_2 to boil as hydrostatic pressure is released on the entire water column. The recipe for a short eruption interval is the same as before but with a shorter heating time for S_3 (compare S_3 in Figs. 5 and 7).

In the case of the long eruptions, the Rayleigh preplay distribution (mode = 9 min.) is superimposed on an 85-minute heating phase and a 55-minute heating phase for short eruptions, producing the composite distribution shown in Figure 8. The agreement with the observed data (Fig. 1A) is quite good, with a subsidiary mode at ~60 minutes for short eruption intervals and a mode at ~92 minutes for long eruption intervals. The physical cause of short-duration eruptions remains unresolved.

DISCUSSION

An alternative model with a conduit geometry based on that illustrated by Hutchinson et al. (1997) yields very similar results to those presented here, indicating that the model is not particularly sensitive to the conduit geometry. On the other hand, the model is quite sensitive to parameters such as the absolute value of the source temperature and the recharge temperature—changes as small as ±20% in these values produce a substantially worse fit to the data of Birch and Kennedy (1972); these temperatures, however, are reasonably well constrained.

Changes in the value of the convective heat transfer coefficient (h) of ±20% also produce substantially worse fits to the data. The value we chose (based on $\Delta T = 10$ °C) is slightly above the middle of the experimental range for the nucleate boiling regime (Incropera and DeWitt, 2005, p. 598). Lastly, Hutchinson et al. (1997) suggested that CO_2 may be present in the conduit water
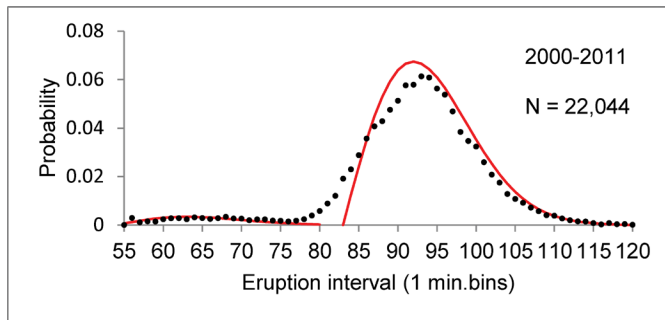
Figure 8. By adding 55 min. (short eruption heating time) and ~85 min. (long eruption heating time) to the preplay Rayleigh distribution (Eq. [1], with a mode of 9 min.; solid curves), the distribution of short and long eruption intervals are reproduced quite well for the period 2000–2011. The circular symbols are the same data as in Figure 1A. Because short eruptions occur about 5% of the time, the Rayleigh probability was scaled by a factor of 0.05 relative to long eruption intervals.

with a pressure of up to 0.2 bars (20 kPa), which would act to lower the reference boiling curve. On Figure 6, this corresponds to ~2 m of hydrostatic pressure and would bring the reference curve closer to the *P-T* conditions in the conduit by this amount (equivalent to 3000 liters of water). The overall effect would be equivalent to shortening the preplay phase (and the eruption interval) by a few minutes.

ACKNOWLEDGMENTS

REFERENCES CITED

Abd-Elfattah, A.M., 2011, Goodness of fit test for the generalized Rayleigh distribution with unknown parameters: Journal of Statistical Computation and Simulation, v. 81, p. 357–366, doi: 10.1080/00949650903348155.

Allen, E.T., and Day, A.L., 1935, Hot Springs of the Yellowstone National Park: Washington, D.C., Carnegie Institute of Washington Publication 466, 525 p.

Birch, F., and Kennedy, G.C., 1972, Notes on geyser temperatures in Iceland and Yellowstone National Park, *in* Heard, H.C., Borg, I.Y., Carter, N.L., Raleigh, C.B., eds., Flow and fracture of rocks: Washington D.C., American Geophysical Union Geophysical Monograph Series, v. 16, p. 329–336.

Bloss, D.F., and Barth, T., 1949, Observations on some Yellowstone geysers: GSA Bulletin, v. 60, p. 861–886, doi: 10.1130/0016-7606(1949)60[861:OOSYG]2.0.CO;2.

Cros, E., Roux, P., Vandemeulebrouck, J., and Kedar, S., 2011, Locating hydrothermal acoustic sources at Old Faithful Geyser using matched field processing: Geophysical Journal International, v. 187, p. 385–393, doi: 10.1111/j.1365-246X.2011.05147.x.

Dowden, J., Kapadia, Brown, G., and Rymer, H., 1991, Dynamics of a geyser eruption: Journal of Geophysical Research, v. 96, p. 18,059–18,071.

Fournier, R.O., 1969, Old Faithful: A physical model: Science, v. 163, p. 304–305, doi: 10.1126/science.163.3864.304.

Fournier, R.O., 1979, Geochemical and hydrological considerations and the use of enthalpy-chloride diagrams in the prediction of underground conditions in hot-spring systems: Journal of Volcanology and Geothermal Research, v. 5, p. 1–16, doi: 10.1016/0377-0273(79)90029-5.

Geis, F., Jr., 1968, Old Faithful: A physical model: Science, v. 160, p. 989–990, doi: 10.1126/science.160.3831.989.

GOSA, 2011, Old Faithful Visitor Center Logs: Geyser Observation and Study Association (GOSA), http://gosa.org/ofvclogs.aspx (last accessed 12 Mar. 2013).

Hayden, F.V., 1872, Preliminary report of the United States Geological Survey of Montana and portions of adjacent Territories; being a fifth annual report of progress: Part I: Washington, D.C., U.S. Government Printing Office, p. 13–204.

Hurwitz, S., Kumar, A., Taylor, R., and Heasler, H., 2008, Climate-induced variations of geyser periodicity in Yellowstone National Park, USA: Geology, v. 36, p. 451–454, doi: 10.1130/G24723A.1.

Husen, S., Taylor, R., Smith, R.B., and Healser, H., 2004, Changes in geyser eruption behavior and remotely triggered seismicity in Yellowstone National Park produced by the 2002 M7.9 Denali fault earthquake, Alaska: Geology, v. 32, p. 537–540, doi: 10.1130/G20381.1.

Hutchinson, R.A., 1985, Hydrothermal changes in the Upper Geyser Basin, Yellowstone National Park, after the 1983 Borah Peak, Idaho, earthquake, *in* Stein, R.S., and Bucknam, R.C., eds., Proceedings of Workshop 28 on the 1983 Borah Peak, Idaho, Earthquake: U.S. Geological Survey Open-File Report 85-290-A, p. 612–624.

Hutchinson, R.A., Westphal, J.A., and Kieffer, S.W., 1997, In situ observations of Old Faithful Geyser: Geology, v. 25, p. 875–878, doi: 10.1130/0091-7613 (1997)025<0875:ISOOOF>2.3.CO;2.

Incropera, F.P., and DeWitt, D.P., 2005, Fundamentals of Heat and Mass Transfer, 5th edition: New York, Wiley, 1008 p.

Ingebritsen, S.E., and Rojstaczer, S.A., 1993, Controls on geyser periodicity: Science, v. 262, p. 889–892, doi: 10.1126/science.262.5135.889.

Kedar, S., Sturtevant, B., and Kanamori, H., 1996, The origin of harmonic tremor at Old Faithful geyser: Nature, v. 379, p. 708–711, doi: 10.1038/379708a0.

Kedar, S., Kanamori, H., and Sturtevant, B., 1998, Bubble collapse as the source of tremor at Old Faithful Geyser: Journal of Geophysical Research, v. 103, p. 24,283–24,299, doi: 10.1029/98JB01824.

Kieffer, S.W., 1984, Seismicity at Old Faithful geyser: An isolated source of geothermal noise and possible analogue of volcanic seismicity: Journal of Volcanology and Geothermal Research, v. 22, p. 59–95, doi: 10.1016/0377-0273(84)90035-0.

Kieffer, S.W., 1989, Geologic nozzles: Reviews of Geophysics, v. 27, p. 3–38, doi: 10.1029/RG027i001p00003.

Murty, T.S., 1979, A mathematical model for pre-boiling convection in a geyser vent: American Journal of Science, v. 279, p. 989–992, doi: 10.2475/ajs .279.8.989.

Rinehart, J.S., 1965, Earth tremors generated by Old Faithful: Science, v. 150, p. 494–496, doi: 10.1126/science.150.3695.494.

Rinehart, J.S., 1969, Thermal and seismic indications of Old Faithful Geyser's inner working: Journal of Geophysical Research, v. 74, p. 566–573, doi: 10.1029/JB074i002p00566.

Rinehart, J.S., 1972, Fluctuations in geyser activity caused by variations in earth tidal forces, barometric pressure, and tectonic stress: Journal of Geophysical Research, v. 77, p. 342–350, doi: 10.1029/JB077i002p00342.

Rinehart, J.S., 1980, Geysers and Geothermal Energy: New York, Springer-Verlag, 222 p.

Smith, E.B., 2005, Basic Chemical Thermodynamics, 5th edition: London, Imperial College Press, 166 p.

Steinberg, G.S., 1980, The enthalpy of the heat-carrying fluids and the energy of eruption of Velican Geyser, Kamchatka: Journal of Volcanology and Geothermal Research, v. 8, p. 267–283, doi: 10.1016/0377-0273(80)90108-0.

Steinberg, G.S., Merzhanov, A.G., and Steinberg, A.S., 1978, Hydrosounding as a method of study of the critical parameters of the geyser: Journal of Volcanology and Geothermal Research, v. 3, p. 99–119, doi: 10.1016/0377-0273(78)90006-9.

White, D.E., 1967, Some principles of geyser activity, mainly from Steamboat Springs, Nevada: American Journal of Science, v. 265, p. 641–684, doi: 10.2475/ajs.265.8.641.

White, D.E., Fournier, R.O., Meffler, J.P., and Truesdell, A.H., 1975, Physical results of research drilling in the thermal areas of Yellowstone National Park, Wyoming: U.S. Geological Survey Professional Paper 892, p. 1–69.